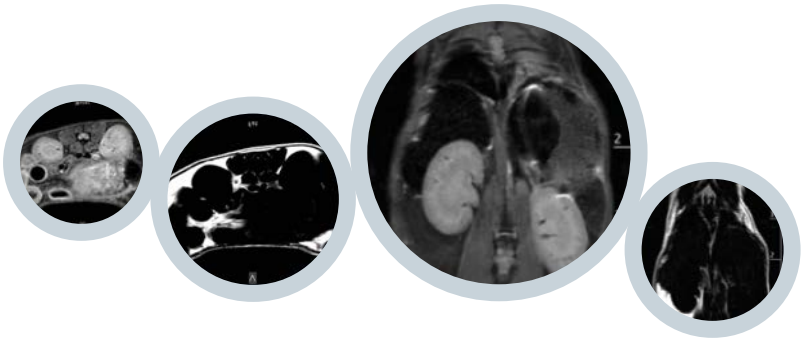

Fat-Water Separation Imaging in Preclinical MRI

Johannes Schneider, Klaus Strobel, and Thomas Basse-Lüsebrink

Bruker BioSpin MRI GmbH, 76275 Ettlingen, Germany

Abstract

Non-invasive *in vivo* phenotyping of adipose tissue deposits in small animal models is of great importance in preclinical metabolic research. Additionally, in Magnetic Resonance Imaging (MRI), fat suppression is often performed with Radio-Frequency (RF) pulse-based fat saturation techniques to avoid artifacts arising from fat. However, RF-based fat suppression can be non-optimal especially at low magnetic fields with low chemical shifts between fat and water as well as at high fields which often have challenging shim conditions. To overcome these limitations an easy to use method to discriminate fat and water in preclinical MRI research is presented. The fully integrated method is introduced with the new ParaVision version: ParaVision 360.

Introduction

Evidence shows that in rodent models both white adipose tissue (WAT) and brown adipose tissue (BAT) play active roles in numerous physiological and pathophysiological processes (Summers 2006). WAT is the physiological site of energy storage, functioning as insulation and providing a protective cushion. BAT is the primary site of non-shivering thermogenesis during cold acclimatization. Importantly, the accumulation of excess WAT has been shown to play a crucial role in the development of cardiovascular, metabolic, and renal disorders, including insulin resistance, diabetes mellitus, hyperlipidemia, atherosclerosis, hypertension, and chronic renal disease, many of which are interdependent. On the other hand, BAT in rodents significantly contributes to prevent obesity and insulin resistance.

Thus, non-invasive *in vivo* phenotyping of adipose tissue deposits in small animal models during the initiation, progression, and manifestation of obesity and obesity-related disorders is necessary in preclinical metabolic research. Currently, dedicated MRI techniques applied to small laboratory animals developing obesity for example are able to provide distribution information of different fat deposits.

Furthermore, these techniques could be used to evaluate disease-related presence and accumulation of lipids in multiple organs (e.g., liver, brain, and kidney) or in the skeletal musculature *in vivo* (Garbow 2004, Brix 1993, Schick 1993).

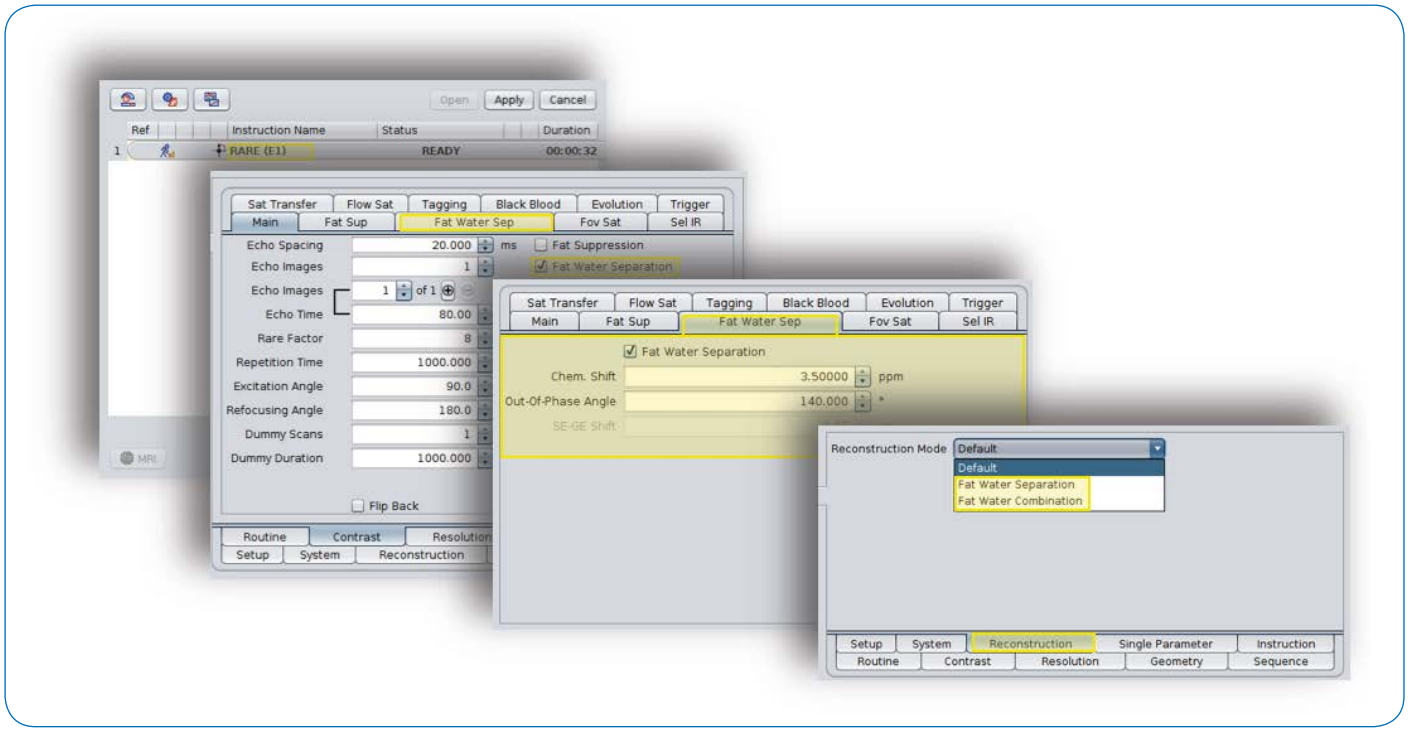

Figure 1: The fat-water separation module in RARE in ParaVision 360. From top-bottom: (1) RARE method in the scan list, (2) Fat-water separation module is activated on the contrast card, (3) detailed parameters can be adjusted for the fat-water separation module, (4) fat and water separated images or a fat and water combined image can be calculated.

Moreover, to avoid artifacts arising from fat in MRI, fat suppression is often performed with RF pulse-based fat saturation techniques. However, RF-based fat saturation can be non-optimal especially at low magnetic fields where the chemical shift between fat and water is low. Thus, saturation of the water peak by the fat suppression RF pulse often cannot be avoided. On the other hand, and especially at high fields, non-perfect shim conditions can lead to an insufficient fat saturation by RF-based techniques (Delfaut 1999).

Here we present a robust, easy to use method to discriminate fat and water in preclinical MRI research which is fully integrated into ParaVision 360.

Fat-water technique

The presented fat-water separation technique is based on the principle described by Dixon in 1984 (Dixon 1984). By exploiting the chemical shift between fat and water, two images are acquired, one with magnetization vectors from fat and water being in-phase and one with the vectors being out-of-phase. Comparing the images' phase distributions, allows separation of the signal contributions of the two components in each pixel.

Afterwards, the components need to be identified either as fat or as water. Since B_0 inhomogeneities additionally influence the signal phase, images with ambiguous or swapped fat and water regions may result. This challenge is mastered by assigning the components to the fat and water images in such a way that a concurrently calculated B_0 map varies smoothly.

The acquisition and reconstruction functionality described above is now available within the Bruker RARE method and thus directly in ParaVision 360. Benefiting from the rapid spin echo train readout, fat and water in-phase images can be acquired in a standard echo train. To acquire out-of-phase

images, another echo train follows with the readout window shifted slightly behind the echo center letting the fat and water magnetization accumulate the desired phase difference.

Typically, echo time shifts are well below 1 ms and thus T_2 and T_2* effects between in-phase and out-of-phase images are neglectable. Consequently, no further images are required and therefore, robust fat water separation is achieved from only two acquisitions, minimizing measurement times and reducing sensitivity to motion and artifacts.

Finally, the reconstruction output can be chosen to generate two separate images of fat and water, respectively. Additionally, a re-combined fat-water image can be reconstructed with correction of the apparent spatial shift of the fat signal, particularly typical in high field MRI.

Figure 1 shows typical steps to generate fat-water separated images in ParaVision 360.

Experimental setup

In vivo and *ex vivo* animal experiments were performed on mice and rats. The study was approved by the local Ethical Committee for Animal Experiments (Regierungspräsidium Karlsruhe).

MRI Systems

Experiments were performed at three different magnetic field strengths: 3 Tesla, 7 Tesla, and 9.4 Tesla (all BioSpec® MRI instruments), Bruker BioSpin MRI GmbH, Ettlingen, Germany.

Anesthesia and physiological monitoring for *in vivo* experiments:

Anesthesia: 1.0-2.0% Isoflurane in an air/O_2 mixture with flow rates of 500 ml/min each was used. Monitoring: Respiration rate and body temperature were monitored using an MR compatible small animal monitoring and gating system (Model 1025, SA Instruments, Inc., Stony Brook, NY, USA). Animals were placed prone on the animal cradle and a stable body temperature was maintained by warm water heating.

Imaging protocol and sequence parameters:

9.4 T *in vivo* rat experiments. Acquisition details: TE: 23 ms, TR: 1800 ms, FOV: (112x90) mm^2, Matrix size: 320x256, Resolution: (350x350) μm^2, Slices: 15, Slice thickness: 1.5 mm, NA: 4, TA: > 3m 50s, resp. trig. per slice. For the out-of-phase image an angle of 140° between fat and water magnetization was chosen, resulting in an echo time shift of 0.28 ms. Coil setup: a circular polarized birdcage coil with an inner diameter of 86 mm was used for signal transmission and reception.

7 T *in vivo* mouse experiments. Acquisition details (Left/Right in Figure 3): TE: 24 ms, TR: 350/402 ms, FOV: (80x36) mm^2 /, (36x27) mm^2, Matrix size: 384x192 / 256x192, Resolution: (0.208x0.188) μm^2 / (0.141x0.141) μm^2, Slices: 5/6, Slice thickness: 1 mm, NA: 4, TA: > 1m 7s / 2m 35s, resp. trig. per slice. For the out-of-phase image an angle of 140° between fat and water magnetization was chosen, resulting in an echo time shift of 0.37 ms. Coil setup: a circular polarized birdcage coil with an inner diameter of 72 mm was used for signal transmission.

3 T *ex vivo* rat experiments. Acquisition details: TE: 48 ms, TR: 1100 ms, FOV: (80x80) mm^2, Matrix size: 256x256, Resolution: (313x313) µm2, Slices: 7, Slice thickness: 1 mm, NA: 16, TA: 9m 24s. For the out-of-phase image an angle of 140° between fat and water magnetization was chosen, resulting in an echo time shift of 0.89 ms. Coil setup: A circular polarized birdcage coil with an inner diameter of 82 mm was used for signal transmission and reception.

Results

The presented technique was able to produce artifact free fat and water images at multiple different field strength for both mice and rats (Cf. Figure 2-4).

For comparison with conventional techniques, fat suppressed images were additionally created by a RF pulse saturation-based technique. Under challenging conditions (e.g. large objects, high fields, non-optimal shim) phase-based fat-water separation techniques outperform RF-saturation-based techniques. Thus, RF-based techniques fail to suppress the fat signal in non-ideal shim conditions (Cf. Figure 2 & 4).

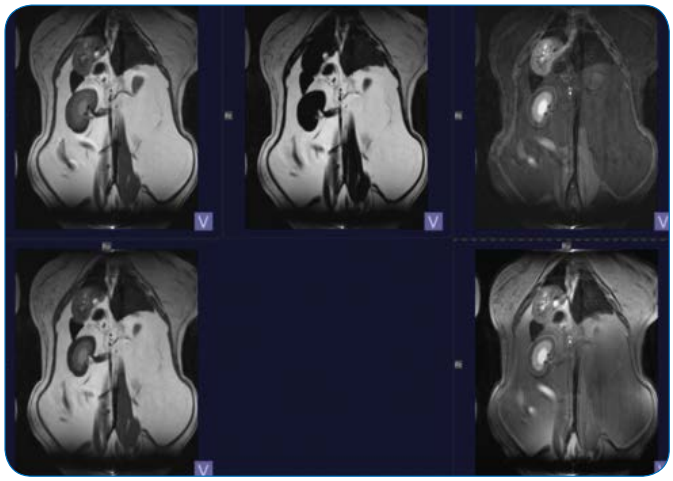

Figure 2: BioSpec 94/20. Upper row: Left, default RARE. Middle, fat image. Right, water image. Lower row: Left, Combined, chemical-shift corrected fat-water image. Right, default RF-based fat saturation image.

Furthermore, since the chemical shift is exactly known for the given field strength, the fat-water separation technique enables chemical shift-free combination images which can be automatically calculated by ParaVision 360 (Cf. Figure 2 & 4).

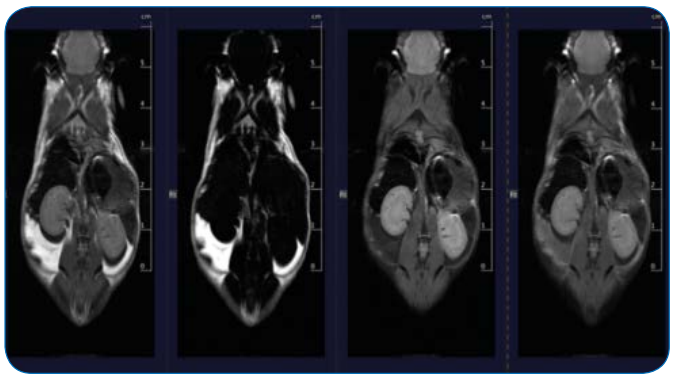

Figure 3A: BioSpec 70/30. Coronal images. From left to right: Default RARE, fat image, water image, default RF-based fat saturation image

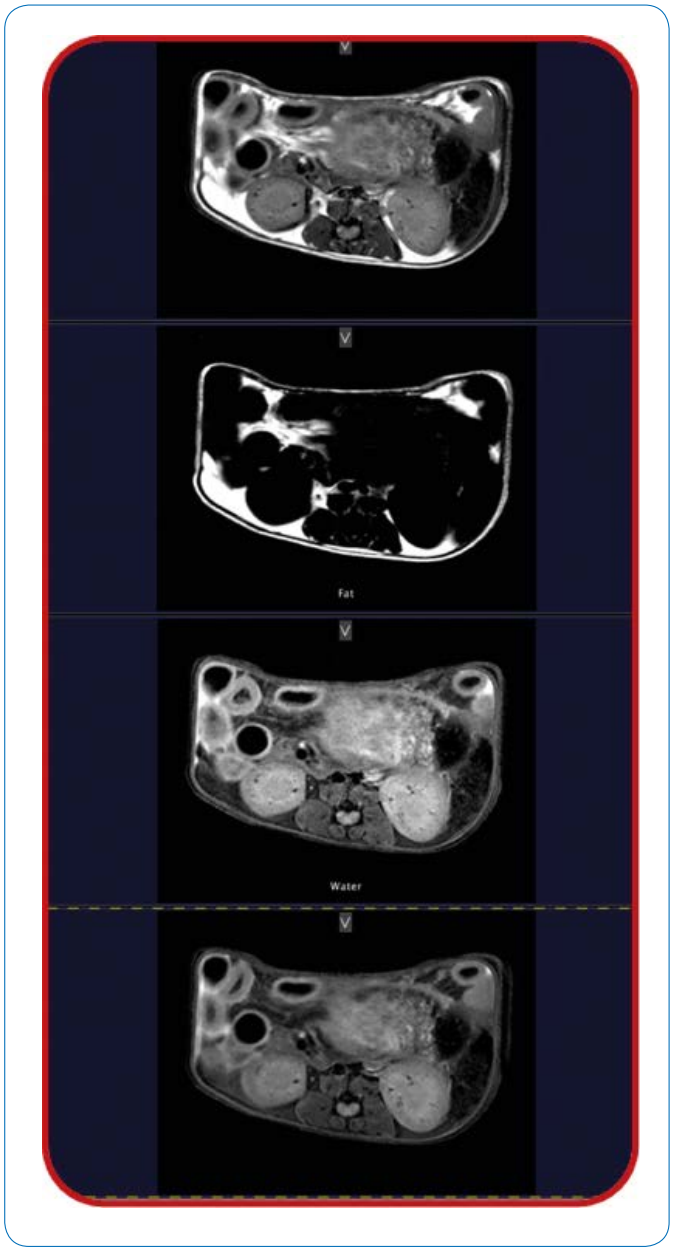

Figure 3B: BioSpec 70/30. Axial images. From top to bottom: Default RARE, fat image, water image, default RF-based fat saturation image

Discussion

A fast and robust fat-water separation technique which is fully integrated into ParaVision 360 was presented.

Besides fat or water only images the technique is capable of automatically calculating chemical shift corrected images. Furthermore, experiments in different conditions showed that the technique is applicable for preclinical MRI experiments at multiple field strengths and different animals. A further benefit of the method is its speed: only two images are needed, one in-phase and one out-of-phase image to calculate the fat and water images, while being robust vs. magnetic field inhomogeneity, which becomes more prominent at higher field.

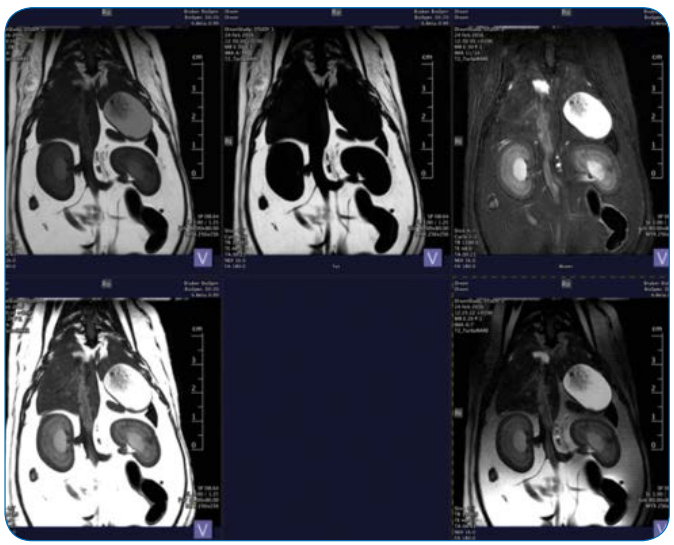

Figure 4: BioSpec, 3 Tesla. Upper row: Left, default RARE. Middle, fat image. Right, water image. Lower row: Left, combined

References

- L. K. Summers, 2006. Adipose tissue metabolism, diabetes and vascular disease—lessons from in vivo studies. Diabetes Vasc. Dis. Res. 3: 12–21.
- J. R. Garbow, X. Lin, N. Sakata, Z. Chen, D. Koh, and G. Schonfeld. 2004. In vivo MRS measurement of liver lipid levels in mice. J. Lipid Res. 45: 1364–1371.
- G. Brix, S. Heiland, M. E. Bellemann, T. Koch, and W. J. Lorenz. 1993. MR imaging of fat-containing tissues: valuation of two quantitative imaging techniques in comparison with localized proton spectroscopy. Magn. Reson. Imaging. 11: 977–991.
- F. Schick, B. Eismann, W. I. Jung, H. Bongers, M. Bunse, and O. Lutz. 1993. Comparison of localized proton NMR signals of skeletal muscle and fat tissue in vivo: two lipid compartments in muscle tissue. Magn. Reson. Med. 29: 158–167.
- E. M. Delfaut, J. Beltran, G. Johnson, J. Rousseau, X. Marchandise, A. Cotten. 1999. Fat Suppression in MR Imaging: Techniques and Pitfalls. RadioGraphics 19: 373–382.
- W. T. Dixon. Simple proton spectroscopic imaging. 1984. Radiology 153: 189-194

Bruker BioSpin

www.bruker-biospin.com/MRI

© Bruker BioSpin